

A disposable, continuous-flow polymerase chain reaction device: design, fabrication and evaluation

Victoria Ragsdale¹ · Huizhong Li² · Himanshu Sant² · Tim Ameel² · Bruce K. Gale²

Published online: 9 July 2016
© Springer Science+Business Media New York 2016

Abstract Polymerase Chain Reaction (PCR) is used to amplify a specific segment of DNA through a thermal cycling protocol. The PCR industry is shifting its focus away from macro-scale systems and towards micro-scale devices because: micro-scale sample sizes require less blood from patients, total reaction times are on the order of minutes opposed to hours, and there are cost advantages as many microfluidic devices are manufactured from inexpensive polymers. Some of the fastest PCR devices use continuous flow, but they have all been built of silicon or glass to allow sufficient heat transfer. This article presents a disposable polycarbonate (PC) device that is capable of achieving real-time, continuous flow PCR in a completely disposable polymer device in less than 13 minutes by thermally cycling the sample through an established temperature gradient in a serpentine channel. The desired temperature gradient was determined through simulations and validated by experiments which showed that PCR was achieved. Practical demonstration included amplification of foot-and-mouth disease virus (FMDV) derived cDNA.

Keywords PCR · Microfluidics · Continuous flow · Heat transfer · Polycarbonate

1 Introduction

PCR has been largely used as a tool for diagnostics in the medical industry, paternity testing (Pena and Chakraborty 1994), and detection of airborne pathogens (Makino et al. 2001; Cheun et al. 2003) due to its highly-effective and well-established ability to amplify specific segments of DNA. PCR consists of three repeating temperature-dependent reactions: denaturation, annealing and extension. To complete the reaction efficiently, the required temperature and an adequate reaction time are necessary. Traditionally macroscale PCR is accomplished by thermally cycling a large sample between the reaction temperatures. Due to the large thermal mass of the PCR mixture, the required transition and thermal equilibrium time cause this process to be very time consuming. Over the past decade, the trend has changed from traditional macro-PCR to micro-PCR to reduce the total reaction time, reduce sample volume requirements (and increased patient comfort), reduce reagent consumption, and lower manufacturing costs. There are three predominant methods for micro-scale PCR: well-based, shuttle, and continuous flow. Each method is characterized by small sample volume, relatively fast reaction time, and microfabrication-based manufacturing technique.

Well-based PCR was the pioneer of micro-PCR devices (Wittwer et al. 1989; Shoffner et al. 1996; Oda et al. 1998; Hühmer and Landers 2000; Lee et al. 2003; Beard et al. 2011; Ouyang et al. 2011; Lounsbury et al. 2011; Kanai et al. 2011). Reagents are housed in a microwell and the environment temperature changes to enable the reactions. Well-based PCR setup is simple and many different samples can be processed simultaneously by using multiple wells, but heating and cooling the fluid takes a considerable amount of time since the entire container must first be heated and then time is needed to ensure the entire micro-volume reaches the reaction

✉ Bruce K. Gale
bruce.gale@utah.edu

¹ Sandia National Laboratories, Albuquerque, NM, USA

² Department of Mechanical Engineering, University of Utah, 1495 E 100 S Room 1550 MEK, Salt Lake City, UT 84112, USA

temperature. To reduce the time waiting for fluid temperatures to transition between reactions, shuttle PCR allows a micro-volume of PCR reactant to move between three isothermal regions in a single channel and is able to produce reliable amplification results while completing the process faster than well-based PCR (Chiou et al. 2001; Cheng et al. 2005; Chen et al. 2007). The disadvantage is that shuttle PCR relies heavily on specialized MEMS pumps and valves, which can be complex and expensive, to control the location and acceleration of the fluid, and these systems are only capable of cycling one sample at a time.

Continuous flow PCR (CF-PCR) uses pressure driven flow to continuously move a PCR sample in one direction through three temperature regions with a constant flow rate (Kopp et al. 1998; Schneega et al. 2001; Li et al. 2006). CF-PCR has been shown to work effectively with a constant flow rate and an established temperature gradient (Wittwer and Herrmann 1999; Park et al. 2003; Dorfman et al. 2005; Chen et al. 2005). As with the two previous methods being limited by the residence time, continuous flow devices are limited by flow rate. As the flow rate is increased, the effectiveness of PCR is reduced since the PCR mixture is not given sufficient time to reach the required extension phase, which is the slowest phase. The other two phases are nearly instantaneous. With only these minor disadvantages, CF-PCR is able to achieve rapid amplification rates while producing a highly effective output with minimal instrumentation (Crews et al. 2008; Orozco 2009).

The common materials used to create micro-PCR devices are glass and silicon due to their preferable thermal behavior, known surface chemistry, and wide-spread availability. Schneega (Schneega et al. 2001) and Crews (Crews et al. 2008) etched CF-PCR microchannels into glass, taking advantage of the transparency and the rounded channels generated by isotropic etching. Glass, though, is an insulator, so it has somewhat reduced heat transfer compared to some metals and silicon, slowing the potential speed of the reaction. Glass can also be difficult to etch and bond at the microscale, while also requiring surface passivation since the glass channel walls are naturally hydrophilic lending themselves to enzyme and DNA adsorption. Veering away from the challenges of glass and increasing heat transfer to the fluid, microchannels were manufactured in highly conductive silicon wafers then bonded to a flat glass slide [6]. The manufacturing process is similar to that of glass in that a microfabrication facility is used, which is costly both in time and resources. Due to the costs and challenges associated with glass and silicon manufacturing, there has been a movement in the microfluidics field to manufacture devices from polymers. Polymers are inexpensive and can be more easily manufactured. However, polymers naturally absorb hydrophobic materials so greater attention is required to increase surface passivation, and some polymers are not stable at the

common PCR temperatures. PCR has been demonstrated in PMMA (Cheng et al. 2005; Lounsbury et al. 2011), PET (Ouyang et al. 2011), and Zeonex (Cao et al. 2010). None of these polymers have good heat transfer qualities, making their use in CF-PCR problematic, but glass and silicon are too expensive for disposable devices as required in diagnostics and medical applications. Thus there is a need to find a practical way to produce CF-PCR devices in polymers.

The device presented in this study relies on the principles established by Crews (Crews et al. 2008) with his serpentine channel glass CF-PCR device that carries the sample between a hot region (denaturation) located along the top of the chip and a cooler region (annealing) along the bottom of the chip. Extension occurs while the sample is transitioning back to the hot region and is slowed down in time by widening the channel in the appropriate thermal region, as shown in Fig. 1. Instead of making the device from glass, laser ablation is used to cut the CF-PCR microchannels out of a polymer. Using this manufacturing approach and the theory behind Crews' device, a CF-PCR device created in PC is presented that completely eliminates the need for a microfabrication facility and is therefore relatively inexpensive to produce. The objective of this work is to show that PCR can be achieved in a disposable, continuous-flow, polycarbonate device, manufactured using a simple and cost effective laser process, through finite element simulations and validation by several experiments.

2 Material and methods

2.1 Device theory

As the proposed device relies on a continuous flow PCR design and a fixed geometry, the number of PCR reaction cycles must be determined during the design process and cannot be changed after manufacturing. Since sufficient PCR results are typically obtained between 25 and 40 cycles, the device is designed with 25 cycles to give the smallest device footprint possible while still generating reliable results. In this serpentine channel, one cycle is defined from one denaturation temperature to the next, or geometrically from peak to peak as seen in Fig. 1.

Continuous flow PCR implies the fluid is given a constant volumetric flow rate, and since the PCR sample requires more time in the extension phase than in the denaturation and annealing phases, the channel width is varied to allow for regional velocity control since the channel height must remain constant. The dimensions are selected to produce the same channel volume as Crews' device. The channel is given a constant width of 0.5 mm when the sample is traveling from denaturation phase to annealing phase and 1.2 mm through the extension phase to increase the residence time for the extension phase. The neighboring fluid channels are spaced

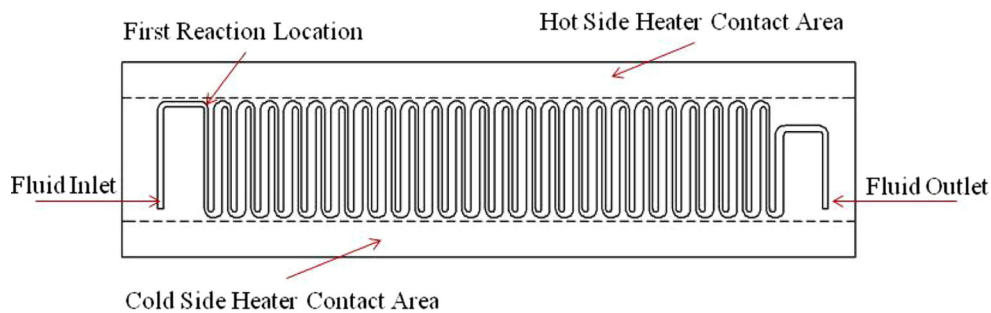


Fig. 1 Schematic diagram of the CF-PCR device topview. Dashed lines represent placement of heaters

0.8 mm apart resulting in the fluid traveling a distance of 33 mm each cycle. Allowing for an approximate 10 mm window of material around the channel geometry, the device footprint area becomes 103.3 x 32.3 mm. The total thickness of this device is approximately 0.33 mm so the channel height is predicted to be 0.11 mm.

With the proposed geometry and a standard flow rate of 1 mL/hr, this device accomplishes PCR by first allowing the fluid to enter and reach the denaturation temperature (90–96 °C) so the double-stranded DNA (ds-DNA) can no longer hold together splitting into two single-stranded DNA (ss-DNA). The fluid then quickly travels down the channel to the annealing temperature (58–65 °C) where primers are attached to the ss-DNA. The ramp rate between denaturation and annealing can happen as fast as the fluid temperature can change, hence the smaller channel width in this region. Also, for most DNA segments these reactions are completed nearly instantaneously once the reaction temperature is reached. The sample continues around the 180° bend and, as it moves back through the thermal gradient, the DNA polymerase seeks the primer locations and begins adding extra nucleotides to the ss-DNA producing a new ds-DNA. Although the extension rate is optimal at an enzyme-specific temperature (72 °C for Taq Polymerase), the reaction is able to occur through a larger temperature range (70–75 °C) (Erlich 1992). A total cycle time of 15 seconds is expected.

2.2 Manufacturing process

The proposed device is made from PC sheets (Lexan FR83) for several reasons. First, PC is a polymer substantially cheaper than silicon or glass. Second, PC is ideal for the laser ablation manufacturing process. Third, PC is available in both opaque and transparent sheets which are essential for real-time fluorescent imaging of the sample as it travels through the device. Unfortunately, PC has low thermal conductivity. Historically, materials with high thermal conductivity, k , such as silicon ($k = 149 \text{ W/m-K}$), have been used in PCR devices. These devices rely on rapid heat transfer through the device

into the fluid and therefore allow shorter residence time. These materials also benefit from a higher specific heat capacity, which essentially means they can more readily store thermal energy. As water (the primary component of a PCR reaction) has a high heat capacity as well, significant energy is required to generate a temperature change. In contrast, the proposed PC CF-PCR device is both less temperature stable, due to the low thermal specific heat capacity and thermal mass, and slower due to its low conductivity ($k = 0.20 \text{ W/m-K}$). To minimize the time required to establish a steady state temperature gradient and allow heat to travel through the polymer from the thermal block below, this device is made as thin as possible to minimize the distance through which heat has to be transferred before reaching the fluid.

The manufacturing process for this microfluidic device is based on a laser laminate ablation process which completely eliminates the need for traditional microfabrication techniques. The device is manufactured from three layers of polycarbonate. The center layer contains the serpentine channel geometry, making the height of the channel entirely dependent on the thickness of the laminate, while the outside layers provide the top and bottom walls to form the PCR device. The channel layer is created by cutting the channel perimeter with a CO₂ laser (Universal Laser Systems, Versa Laser), then using tweezers to remove the volume which will become the channel. This laser is capable of producing smooth edges while maintaining tight tolerances. The top layer is then laminated to the center channel for 3 minutes at 175°C in a heat press. The inlet and outlet holes are cored in the correct position to allow fluid flow then the bottom layer is laminated in the same manner for approximately 2.5 minutes at 175°C. The device is then cut to a rectangle.

With the device laminated together and cut into shape, the last manufacturing step is creating and attaching interfaces to allow the PCR sample to be injected into the system and easily collected at the end. The interfaces are made from Polydimethylsiloxane (PDMS) and then cored and attached to the device using double-sided pressure tape (3M 96042). Since the device has a thickness of only approximately 0.75 mm, it loses heat very easily despite the low conductivity of the PC. To prevent too much heat from escaping the system

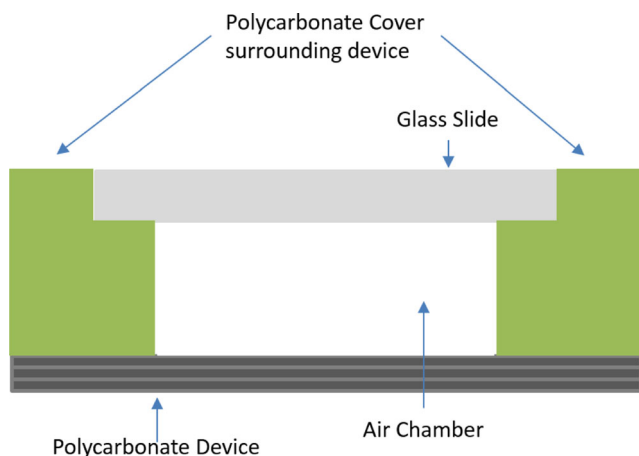


Fig. 2 Schematic diagram of the test setup side view

during testing, the entire device is covered with insulation except the area directly over the fluid channel, which is covered by a removable glass slide to reduce convection from the surface. This removable glass slide, which is offset from the chip by 25.4 mm, allows for the line of sight required for IR temperature measurements while maintaining an air gap which provides adequate insulation when installed. A view from the side, looking perpendicular to the channel, is shown in Fig. 2.

2.3 Simulations

Simulations of the device, coupling heat transfer and fluid dynamics, were completed to demonstrate PC as a suitable material for PCR. The first aim of the study was to show that the fluid sample can reach the required reaction temperatures at various flow rates. The second aim of this study was to estimate the difference in temperature from the center of the fluid channel, where the PCR reactants are, to the top of the device, where the IR camera would measure temperature during experiments. This estimate is critical to calibrating the IR temperature data.

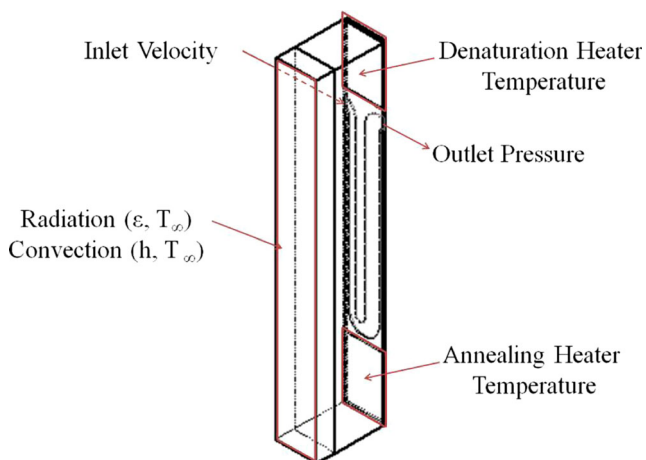


Fig. 3 3D periodic flow simulation boundary conditions

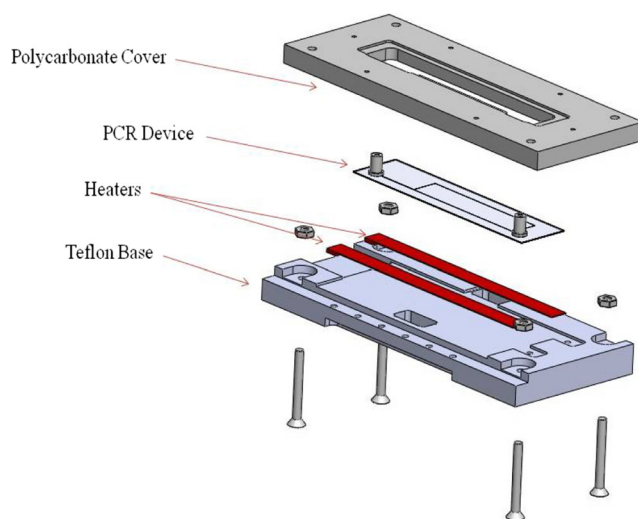


Fig. 4 Experimental fixture showing the arrangement of the heaters, PCR chip, and the cover

To achieve the first aim, a single three-dimensional (3D) PCR loop with periodic flow boundary conditions was modeled with the air gap and glass on top using COMSOL Multiphysics Version 4.2. The physics used for this simulation was ‘conjugate heat transfer,’ which couples the energy and momentum equations allowing simultaneous solution of the the heat transfer and fluid dynamics. The periodic boundary conditions imply that the fluid leaving the device has the same properties as the fluid entering the device, resulting in a model which simulates an infinite number of cycles. A range of appropriate heater set-point temperatures were defined at the heater interface with the device above (denaturation zone) and below (annealing zone) the fluid channel and were optimized for each flow rate to generate the desired temperature. An inlet velocity was defined so the fluid experiences flow rates between 0.1 and 1 mL/hr. Convection and radiation act on the top surface while conduction and radiation act between the device and glass surface. Convection on the top surface is assumed to be low level natural convection, with $h = 2 \text{ W/(m}^2\text{-K)}$. In this model all regions that do not have an isothermal, convection, radiation or periodic boundary condition are considered to be adiabatic. These boundary conditions are summarized in Fig. 3.

Table 1. Summary of temperature set-points used for the different flow rates during experimentation.

Flow Rate [mL/hr]	Heater Temperatures	
	Denaturation [K]	Annealing [K]
0.1	388	327
0.25	385	327
0.5	384	329
1	384	329

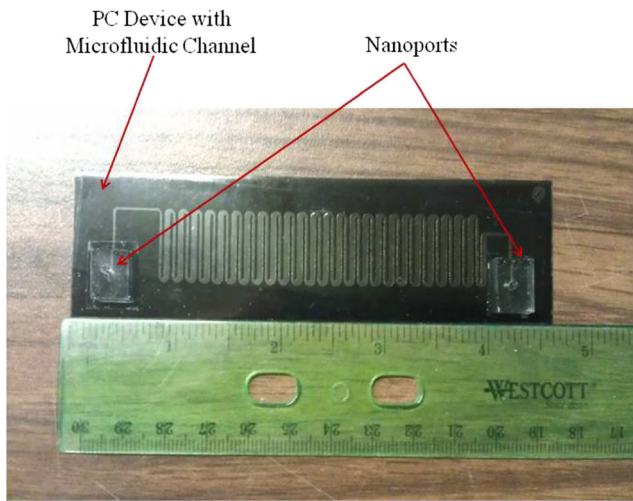


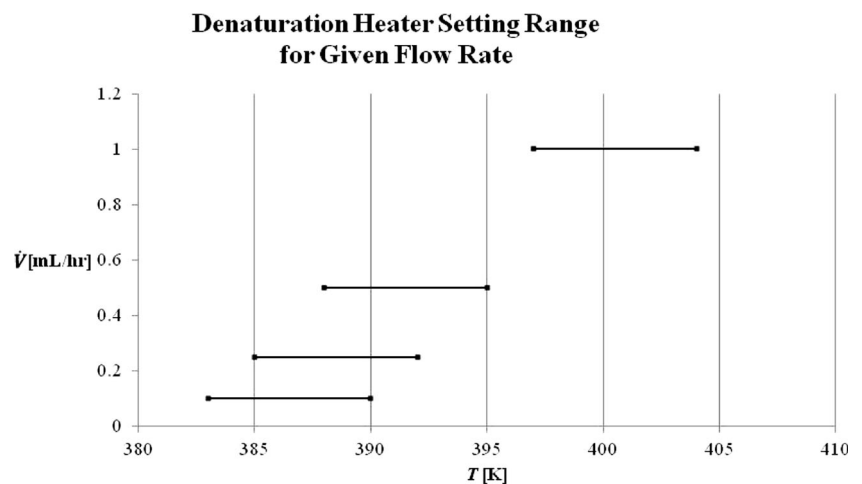
Fig. 5 Photograph of polycarbonate CF-PCR device with custom PDMS ports

The final model included fluid motion and required the mesh to be based on the velocity. A model with 935350 mesh elements was used to analyze the out-of-flow-plane heat transfer. A simulation with 1114638 mesh elements was also solved to verify mesh independence. When the maximum velocity from the two mesh cases resulted in less than 2% error, the solution was assumed to be fully converged. The simulation was completed with four flow rates (0.1 mL/hr, 0.25 mL/hr, 0.5 mL/hr, 1 mL/hr) and heater set-point temperatures were varied by trial-and-error until the simulation predicted that the fluid sample reached the desired PCR temperature ranges in the reaction locations.

2.4 Thermal experiments

Experimental data are needed to validate that the simulation results are correct. A fixture was created to closely match the simulation conditions. To perform the validation experiment, a temperature controller, power supply, syringe pump, IR

Fig. 6 Acceptable heater temperatures on the denaturation side to allow the fluid temperature to reach a value between 90 and 96°C



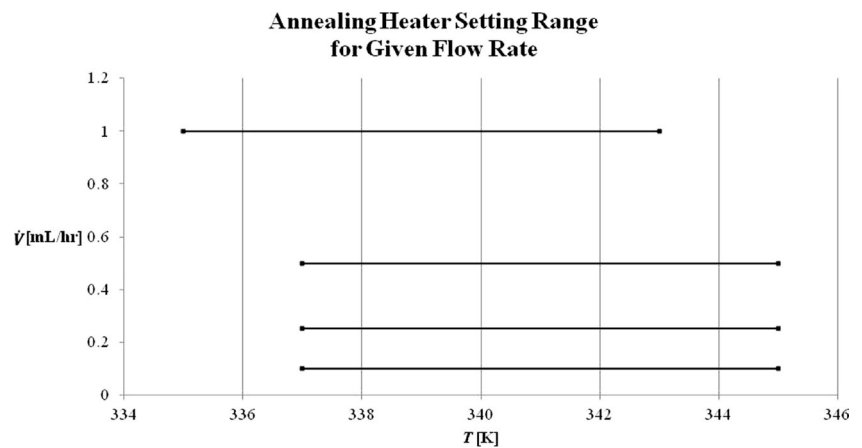
camera, heaters, and temperature sensors were required in addition to the fixture and device. An expanded view of the fixture and device is shown in Fig. 4. The fixture consists of a Teflon piece providing insulation to the bottom of the device, a polycarbonate cover creating insulation around the top of the device, and removable glass slides coated in black spray paint (not shown) closing the gap above the device. The glass slides are spray painted black to increase the emissivity of the glass thereby increasing the accuracy of the IR images of the glass surface. Without the paint, the IR camera image is a composite of the device and the glass. An IR camera was positioned above this fixture. Just before an IR image was taken, the glass slides were removed laterally (to reduce the amount of convection generated above the device) in order to get the most accurate temperature results. The glass slides were then replaced once an image was taken.

The denaturation and annealing heater temperatures were based on the simulation results and summarized in Table 1. The denaturation and annealing heater temperatures varied slightly from the ranges found in the simulation results because at temperatures higher than 388 K, evaporation or bubbles were observed in the channels. The device was allowed to reach steady state before the PCR mixture was pumped through the device at different flow rates. To ensure that a steady-state thermal gradient was achieved, IR images were taken periodically throughout the heating process and the change in maximum temperature recorded. When this temperature change was less than 0.3K over an hour, the device was considered steady state.

2.5 PCR experiments

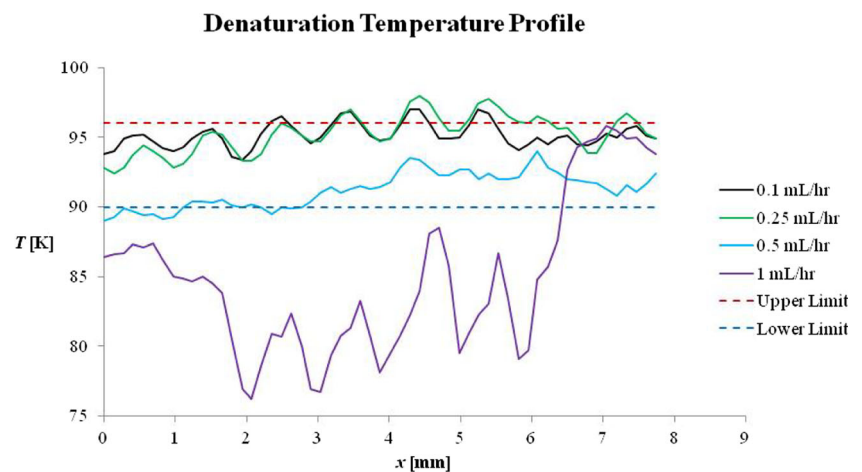
The polycarbonate microfluidic chips were demonstrated by amplifying genetic markers for foot and mouth disease virus

Fig. 7 Acceptable heater temperatures on the annealing side to allow the fluid temperature to reach a value between 58 and 65°C



(FMDV), which is endemic to many parts of Africa and southeast Asia. This work was done in a biosafety 2 lab in India, where FMDV is endemic. A standard spin kit was used to extract viral RNA, convert to cDNA and then amplified using PCR in the polycarbonate chips. We used a PCR chemistry developed by us previously (Sundberg et al. 2010). Universal primers P1 and P2 for FMDV were used to generate an expected amplicon of 202 bp. The PCR chips were loaded with 5 μ L of glycerol, to coat the channels and reduce fouling, followed by 10 μ L of PCR mix. RT was done at 50°C for 30 min followed by 15 min at 95°C for hotstart activation. The heater temperatures for PCR were 368.1 K and 324 K, which were found after some optimization with the PCR mix. Note that the denaturation temperature was somewhat lower than that for the simulations as the cDNA and PCR amplicon melted at a lower temperature than is required for genomic DNA. The PCR mix was pulled through the chip using a syringe pump at a flowrate of 0.5 ml/hr. Standard gel electrophoresis and gel imaging was done to determine the amplicon size. A typical PCR run was less 13 minutes, though some experiments were less than 10 minutes.

Fig. 8 Temperature data across the denaturation bends of the device from experiments with four flow rates. This information takes into account the PC temperature as well as the channel temperature, so the troughs represent the device temperature just above the fluid channel



3 Results and discussion

3.1 Manufacturing results

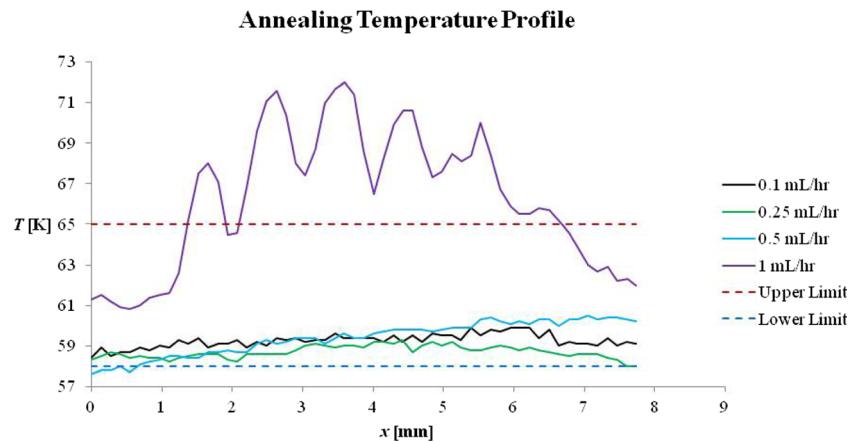
A completed PC device is shown Fig. 5. The entire manufacturing process takes approximately 3 hours, including the 2-hour PDMS curing process for the connections. The average manufacturing time per device can be reduced further since multiple devices can be cut and laminated simultaneously. Using this PC laser lamination process greatly reduces the required time and resources required to build a chip when compared to traditional glass PCR devices.

3.2 Simulation results

The simulation results showed that there were a range of heater set points which would enable PCR to occur, as shown in Figs. 6 and 7.

Figure 6 suggests that as the flow rate increases, the denaturation heater must increase its temperature to achieve the desired reaction temperatures. Intuitively, this makes sense

Fig. 9 Temperature data across the annealing bends of the device from experiments with four flow rates. This information takes into account the PC temperature as well as the channel temperature, so the peaks represent the device temperature just above the fluid channel



since as the velocity increases, less time is given for the fluid to reach the desired temperature before moving onto the next reaction; therefore, there must be a higher heat transfer rate to drive the desired temperature change. Figure 7 shows that for the lower flow rates, the annealing temperature settings and the achieved sample temperature were consistent and did not vary with flow rate significantly. For the fastest simulated flow rate of 1 mL/hr, the required temperature setting was slightly lower, as might be expected, as higher flow rates will require cooler temperatures to cool sufficiently and less time will be available to generate the temperature change. With the device absorbing heat, the desired annealing temperature was achieved without a large dependence on flow rate.

The secondary product of this simulation was the temperature difference between the fluid and the device surface. For flow rates below 0.5 mL/hr, the estimated average temperature difference between the fluid and surface is less than 0.07°C . When the flow rate is increased there is not enough time for the fluid to change temperature resulting in the surface temperature being greater than the fluid temperature on the denaturation side. For 1 mL/hr, the fluid in the denaturation bend is 0.3°C less than the surface temperature. This trend was not noticed on the cold side, most likely due to the decrease in heat loss throughout the center. Even with the largest temperature difference of approximately 0.3°C , the resolution of the IR camera is less than this, so the temperature difference between the center of the fluid channel and the device surface can be

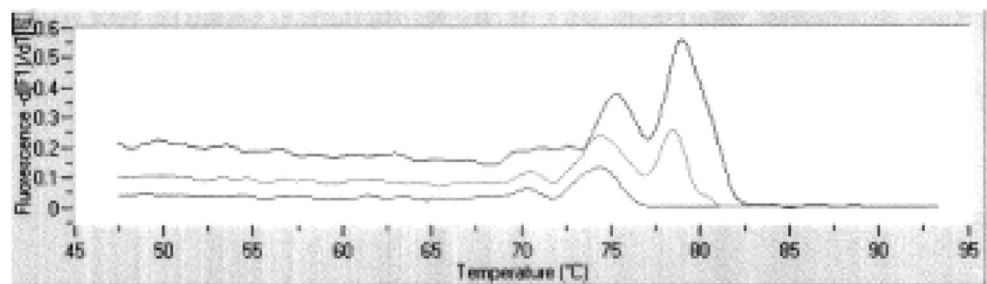
neglected. In other words, the IR surface temperature was assumed to be the fluid temperature.

3.3 Thermal experiments results

The IR temperature readings were analyzed to determine the temperatures across the PCR chip for the heater temperatures that were summarized in Table 1. Measured temperatures from a series of IR images are shown in Figs. 8 and 9 for the denaturation and annealing sides, respectively. The thermal images show that with a flow rate equal to or less than 0.5 mL/hr, the temperatures are within the PCR reaction temperature limits, or could easily be adjusted to fit within the limits. The temperatures used for the 0.5 mL/hr flow rate were on the lower limit of the allowable heater temperature range found in the simulation results so they are expected to be just within the temperature limits. In the denaturation plot, there are two points slightly below the lower temperature limit. This deviation from the simulation is likely due to either the inconsistent flow rate or slightly different lab environmental conditions than those defined in the simulation.

For a flow rate of 1 mL/hr, neither the denaturation nor annealing reaction temperatures are met within the device for the heater temperatures used in the experiment (which were identical to those used for the 0.5 mL/hr experiment). These results are consistent since the predicted heater temperatures required to reach the reaction temperatures for a flow rate of 1 mL/hr were approximately 9°C higher than the

Fig. 10 Melting curves for FMDV PCR amplicon showing the primary peak at 81°C corresponding to the 202 bp amplicon for 3 flow rates



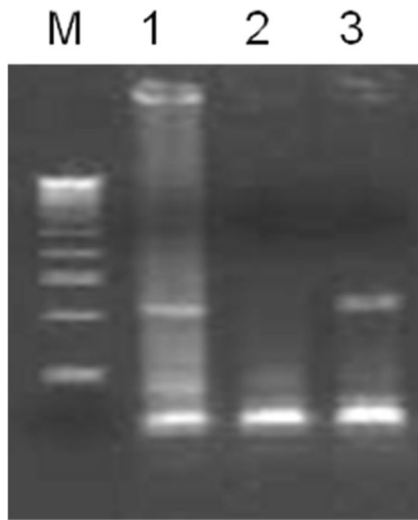


Fig. 11 Image of electrophoresis gel of the PCR product from FMDV viral culture obtained with microfluidic PCR. Lane 1 is OIND R2/75 FMDV strain, Lane 3 is Asia 1 WBN FMDV strain and Lane 2 is negative control

temperatures actually used in the experiments. Overall, for 1 mL/hr, the fluid temperature changed less than 8°C on average between the annealing and denaturation regions suggesting that significantly higher and lower denaturation and annealing heater temperatures would be required for successful PCR. From the simulations, the average temperature difference between these reaction temperatures should be at least 25°C. A difference of less than 8°C suggests that additional heat is being lost and much higher denaturation temperatures than used would be required.

3.4 PCR results

As might be expected from the temperature analysis results, PCR was successfully obtained in the devices in less than 13 minutes at the flow rate of 0.5 mL/hr. To verify that PCR was achieved in the sample that was run through the PC device, a standard melting analysis was completed on the amplicon; the results of which are shown in Fig. 10. The upper graph shows the fluorescence of the amplicon as the temperature was ramped between 45°C and 96°C for three different device temperature settings. The details of this procedure are outlined in Crews' work (Crews et al. 2008). The results show that the main amplicon melting peak could be obtained at ~81°C along with some shorter segments and primer-dimers at lower temperatures. The results suggest that PCR can be successfully completed when optimized for temperature and flow rate (note how the results improve with reduced flow rate).

Figure 11 shows the results of gels run using the amplicon from the PCR chip showing the 202 bp amplicon in lanes 1 and 3 in comparison to the negative (lane 2) control.

Overall, these results validate both the simulation and the ability of the polycarbonate chips to perform PCR.

4 Conclusions

A disposable, polycarbonate CF-PCR device was developed and analyzed in this work. The device is made using xurography from polycarbonate sheets and the sheets are laminated together. This approach results in disposable PCR chips with an almost insignificant manufacturing cost of less than one cent in high volumes. In addition, a periodic simulation was developed and validated which can be used for future refinement of the design and experiments. The simulation produced acceptable results when compared to experimental data for most flow rates, though larger errors developed for high flow rates. It was shown that this device was able to achieve PCR in approximately 13 minutes, though the PCR was only successful for flow rates of less than 0.5 mL/hr. Specifically, the chips were shown to be able to amplify FMDV cDNA, making this chip a practical approach to detecting this disease in countries where the disease is endemic.

Acknowledgements The authors would like to acknowledge Carl Wittwer and his laboratory for help with PCR testing. We also acknowledge Indian Immunologicals Ltd. Hyderabad, India for partial funding towards testing of the microfluidic PCR chip and FMDV viral culture.

Compliance with ethical standards

Funding This study was partially funded by Indian Immunological Ltd., Hyderabad, India.

Conflict of interest The authors declare that they have no conflict of interest.

This article does not contain any studies with human participants or animals performed by any of the authors.

References

- S. R. Beard, et al., Microwell Array PCR Chip for Study of Genetically Engineered Mouse Stem Cells, presented at the MicroTAS, Seattle, Washington, (2011)
- Q. Q. Cao, et al., Plastic microfluidic chip for continuous flow polymerase chain reaction: Simulations and experiments, *Biotechnology Journal*, (2010)
- J. Chen et al., Electrokinetically synchronized polymerase chain reaction microchip fabricated in polycarbonate. *Anal. Chem.* **77**, 658–666 (2005)
- L. Chen et al., Ultrasensitive PCR and real-time detection from human genomic samples using a bidirectional flow microreactor. *Anal. Chem.* **79**, 9185–9190 (2007)
- J. Y. Cheng et al., Performing microchannel temperature cycling reactions using reciprocating reagent shuttling along a radial temperature gradient. *Analyst* **130**, 931–940 (2005)
- H. Cheun et al., Rapid and effective detection of anthrax spores in soil by PCR. *J. Appl. Microbiol.* **95**, 728–733 (2003)
- J. Chiou et al., A closed-cycle capillary polymerase chain reaction machine. *Anal. Chem.* **73**, 2018–2021 (2001)

- N. Crews, C. Wittwer, B. Gale, Continuous-flow thermal gradient PCR. *Biomed. Microdevices* **10**(2), 187–195 (2008)
- K. D. Dorfman et al., Contamination-free continuous flow microfluidic polymerase chain reaction for quantitative and clinical applications. *Anal. Chem.* **77**, 3700–3704 (2005)
- H. A. Erlich, PCR technology: principles and applications for DNA amplification (W.H. Freeman and Company, New York, 1992)
- A. Hühmer, J. Landers, Noncontact infrared-mediated thermocycling for effective polymerase chain reaction amplification of DNA in nanoliter volumes. *Anal. Chem.* **72**, 5507–5512 (2000)
- M. Kanai, et al., A novel contamination free PCR well Array device for clinical applications, presented at the MicroTAS 2011, Seattle, Washington, (2011)
- M. U. Kopp et al., Chemical amplification: continuous-flow PCR on a chip. *Science* **280**, 1046 (1998)
- T. M. H. Lee et al., Microfabricated PCR-electrochemical device for simultaneous DNA amplification and detection. *Lab Chip* **3**, 100–105 (2003)
- S. Li et al., A continuous-flow polymerase chain reaction microchip with regional velocity control. *J. Microelectromech. Syst.* **15**, 223–236 (2006)
- J. A. Lounsbury, et al., A multi-chamber PMMA Microdevice for simultaneous amplification of up to Sevel individual samples using infrared-mediated PCR, presented at the MicroTAS 2011, Seattle, Washington, (2011)
- S. I. Makino et al., Detection of anthrax spores from the air by real-time PCR. *Lett. Appl. Microbiol.* **33**, 237–240 (2001)
- R. Oda et al., Infrared-mediated thermocycling for ultrafast polymerase chain reaction amplification of DNA. *Anal. Chem.* **70**, 4361–4368 (1998)
- R. L. Orozco, Computational heat transfer study of thermal gradient continuous flow polymerase chain reaction devices (University of Utah, Department of Mechanical Engineering, 2009)
- Y. Ouyang, et al., Development of disposable Multichambered microchip PCR via non-contact IR mediated thermal control, presented at the MicroTAS 2011, Seattle, Washington, (2011)
- N. Park et al., Cylindrical compact thermal-cycling device for continuous-flow polymerase chain reaction. *Anal. Chem.* **75**, 6029–6033 (2003)
- S. D. J. Pena, R. Chakraborty, Paternity testing in the DNA era. *Trends Genet.* **10**, 204–209 (1994)
- I. Schneega et al., Miniaturized flow-through PCR with different template types in a silicon chip thermocycler. *Lab Chip* **1**, 42–49 (2001)
- M. A. Shoffner et al., Chip PCR. I. Surface passivation of microfabricated silicon-glass chips for PCR. *Nucleic Acids Res.* **24**, 375 (1996)
- S. Sundberg, C. Wittwer, C. Gao, B. Gale, Spinning disk platform for microfluidic digital polymerase chain reaction. *Anal. Chem.* **82**, 1546–1550 (2010)
- C. T. Wittwer and M. G. Herrmann, Rapid thermal cycling and PCR kinetics, PCR applications: protocols for functional genomics (1999), p. 211
- C. Wittwer et al., Automated polymerase chain reaction in capillary tubes with hot air. *Nucleic Acids Res.* **17**, 4353 (1989)